Supplement of Solid Earth, 12, 463–481, 2021
https://doi.org/10.5194/se-12-463-2021-supplement

Solid Earth Open Access EGU

Supplement of

Crustal structure of southeast Australia from teleseismic receiver functions

Mohammed Bello et al.

Correspondence to: Nicholas Rawlinson (nr441@cam.ac.uk)

Contents

- Introduction
- H-κ stacking analysis
- Figures S1-S4
- 1-D S-wave velocity inversion
- Figures S5-S10

Introduction

This supplementary material presents H- κ stacks and 1-D NA inversion results that are not presented in the main text. It also includes a comparison of Moho depths beneath Tasmania.

H-κ stacking analysis

In this section, results from the H-κ stacking analysis for RFs at stations listed in Table 2 of the main text are presented. In each case, one panel represents the normalised amplitudes of the stack over all back-azimuths along the travel time curves corresponding to the Ps and PpP s + PsPs phases. The other panel is the corresponding stacked receiver function for the station.

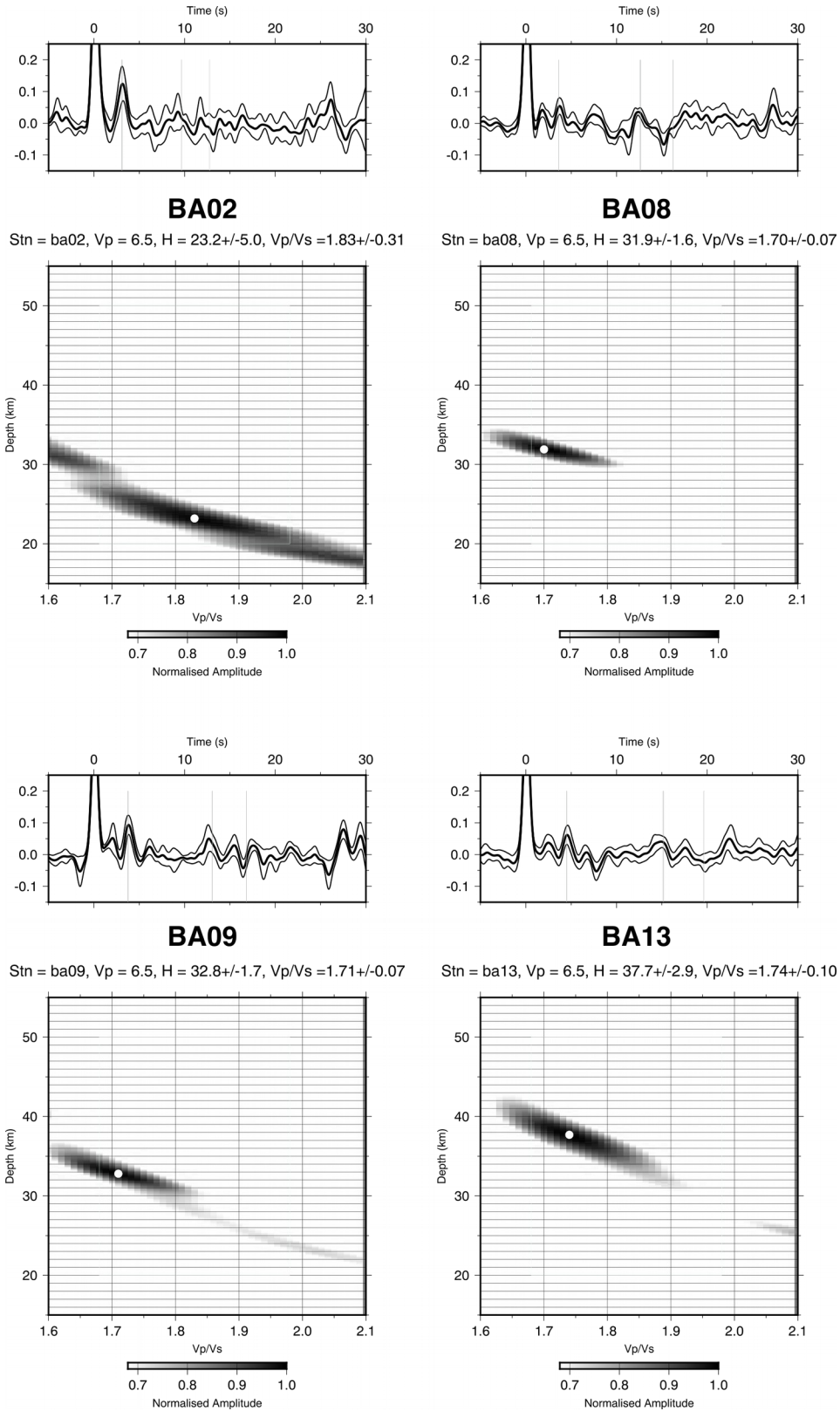

Figure S1: H-κ stacking results for stations BA02, BA08, BA09 and BA13 from the temporary network.

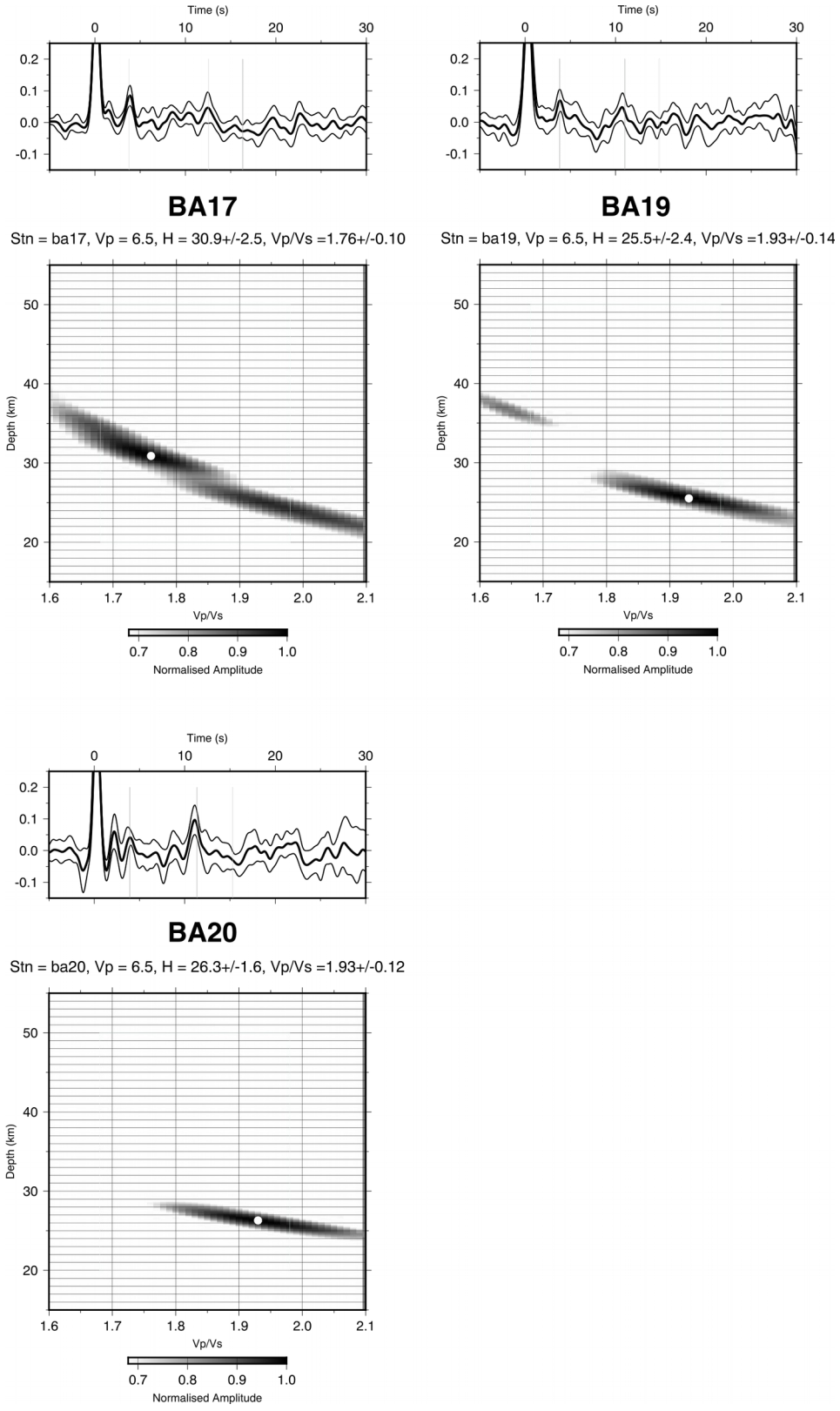

Figure S2: H-κ stacking results for stations BA17, BA19 and BA20 from the temporary network.

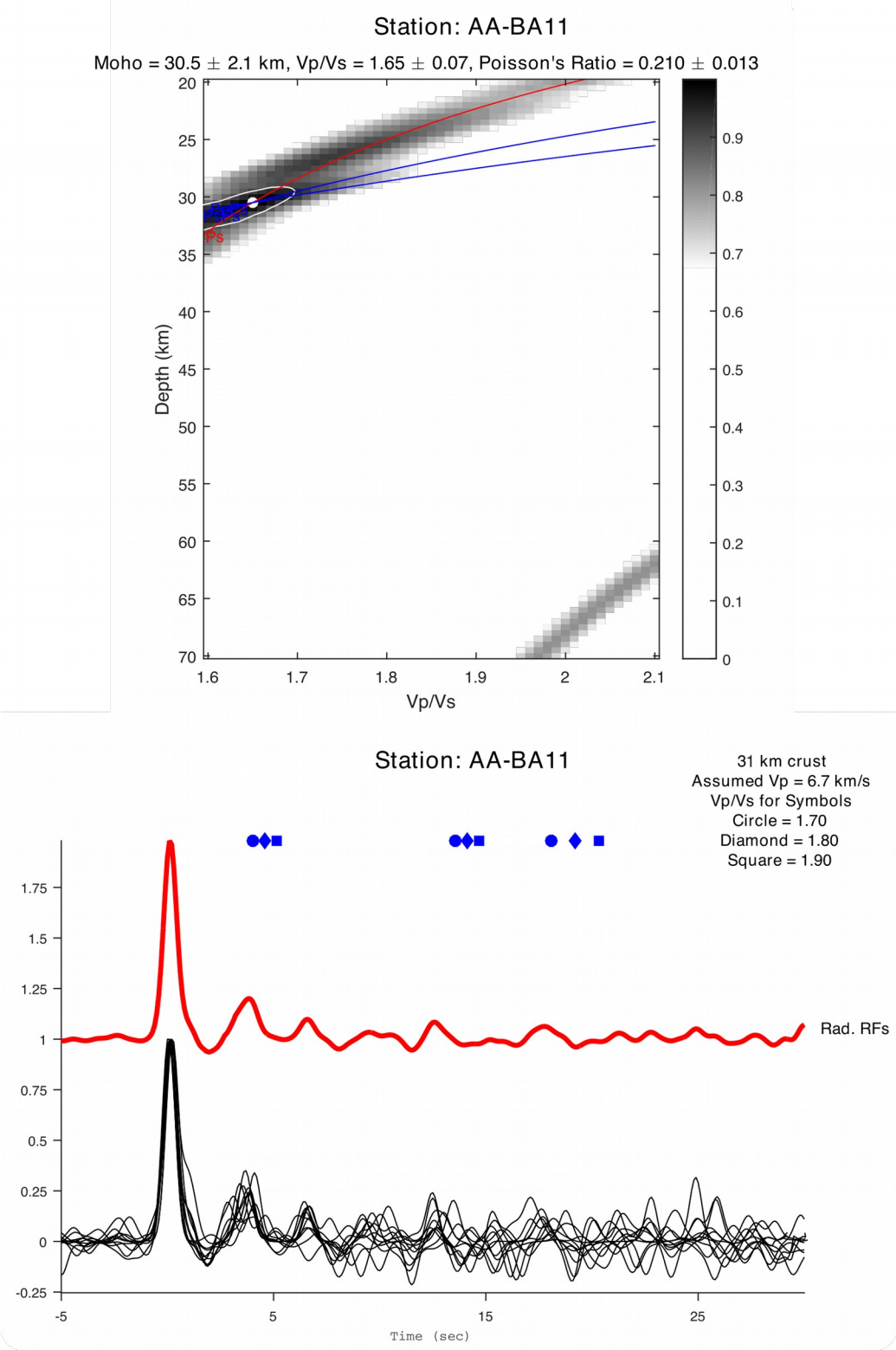

Figure S3: H-κ stacking results for station BA11 from the temporary network.

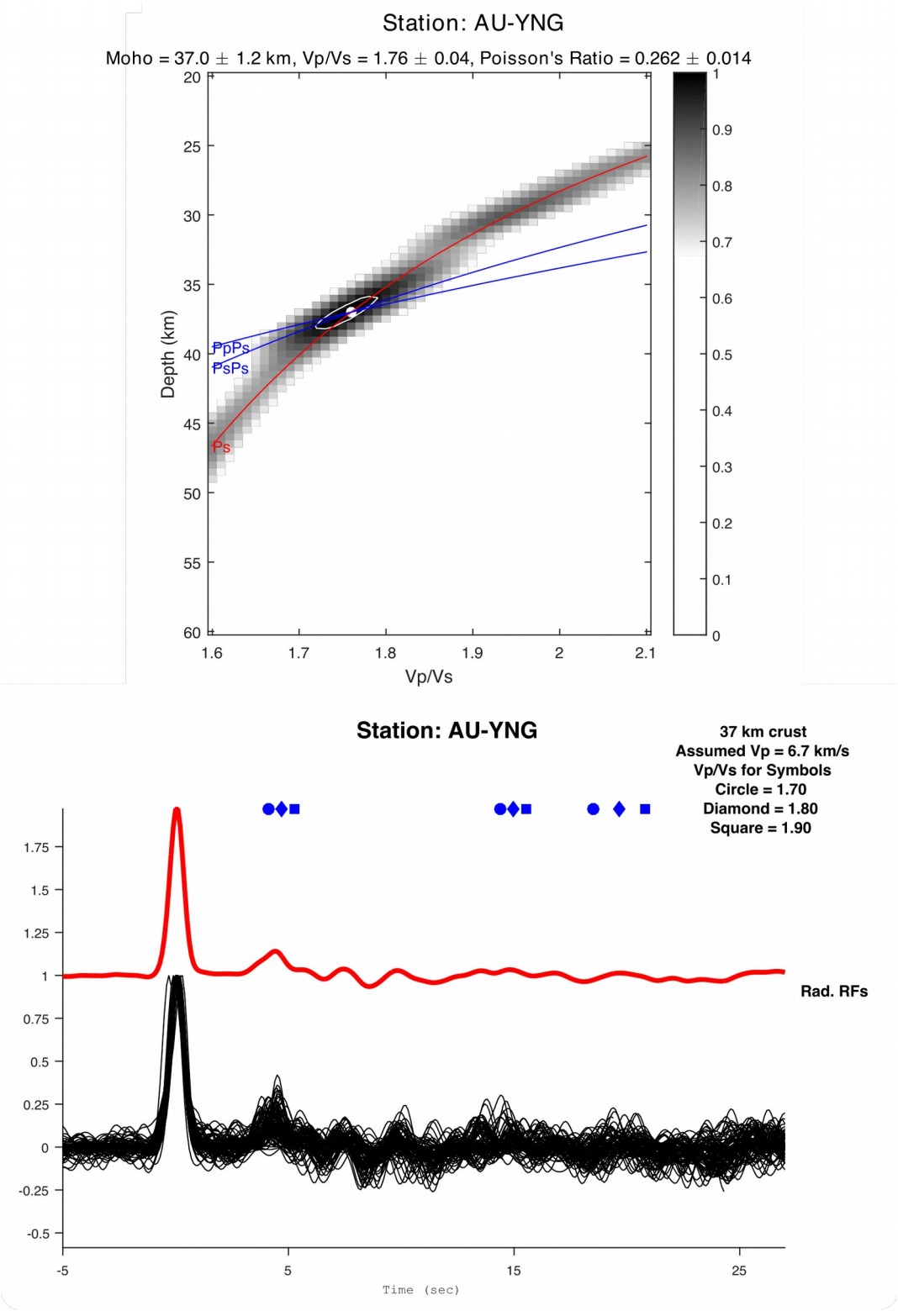

Figure S4: H-κ stacking results for permanent station YNG.

1-D S-wave velocity inversion

This section presents seismic S-wave velocity models for stations listed in Table 2, except those already shown in the main manuscript, obtained from receiver function inversion using the neighbourhood algorithm. The grey area indicates all the models searched by the algorithm. The best 1000 models are indicated in the yellow to green colour; the best model (smallest misfit) corresponds to the red line, both for S-wave velocity and *Vp/Vs* ratio, whereas the white line is the average velocity model computed from the best 1000 models. (Right) Waveform matches between the observed stacked receiver functions (black) and prediction (grey) based on the average of the best 1000 models.

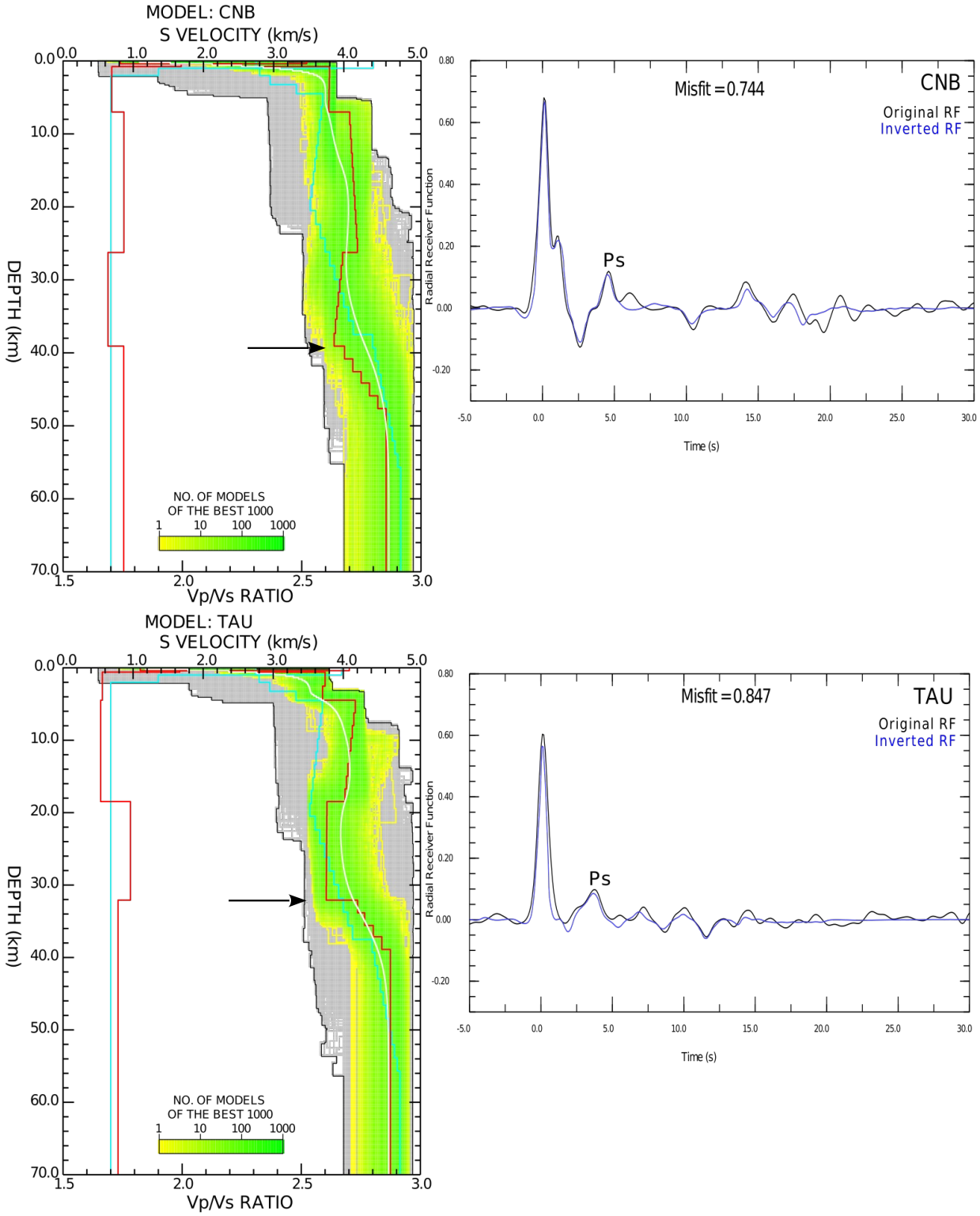

Figure S5: (Left) Density plot of S-wave velocity models and (right) observed and synthetic RF plots for stations CNB and TAU. Small black arrows on the depth profiles denote the estimated depth of the Moho.

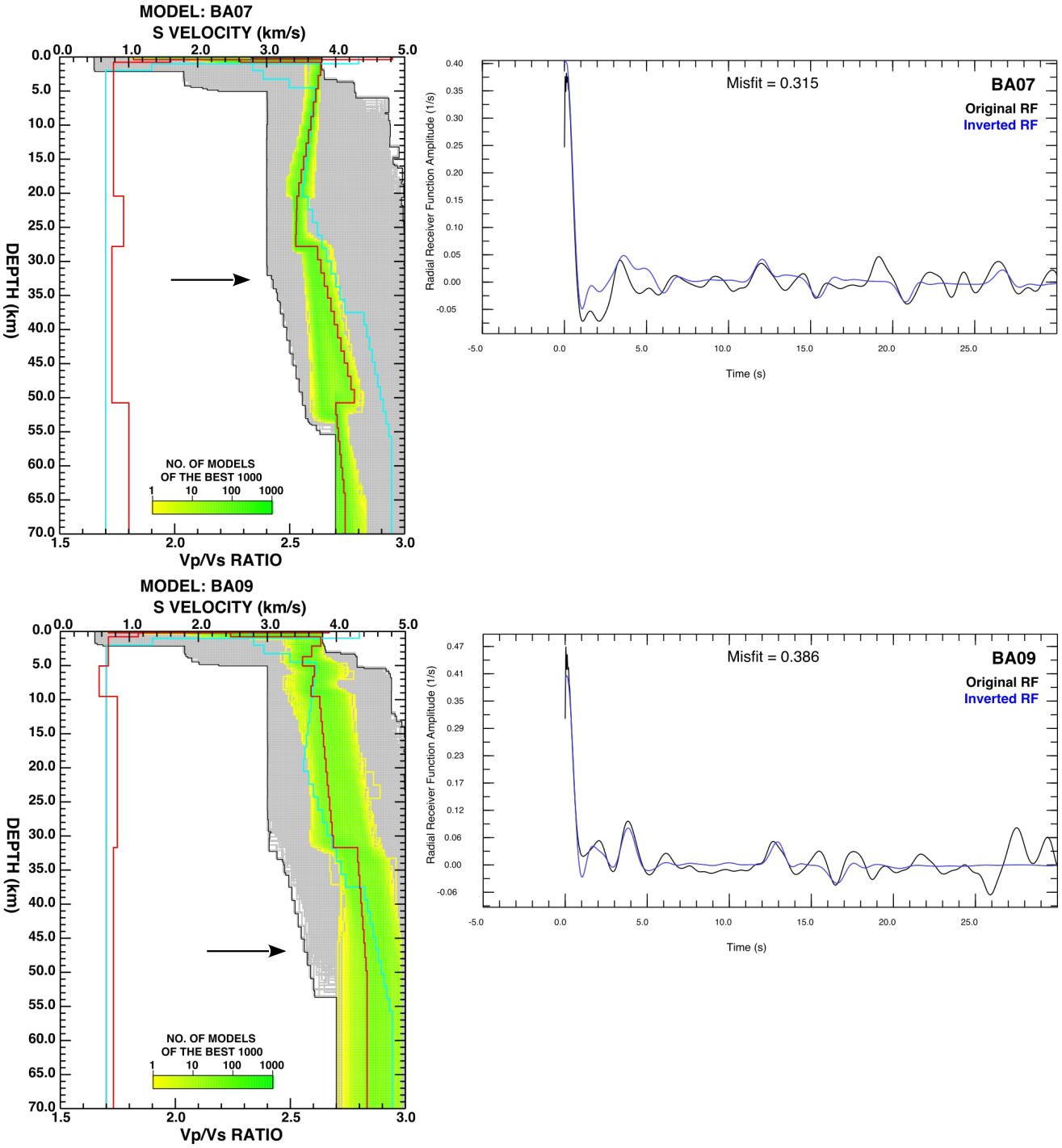

Figure S6: (Left) Density plot of S-wave velocity models and (right) observed and synthetic RF plots for stations BA07 and BA09. Small black arrows on the depth profiles denote the estimated depth of the Moho. Note that receiver function inversion was limited to fitting the waveform between 0 and 30 seconds after the P-arrival for temporary BASS network stations (network code starting with BA) because this produced superior results to the -5 – 30 second time window used for permanent station data.

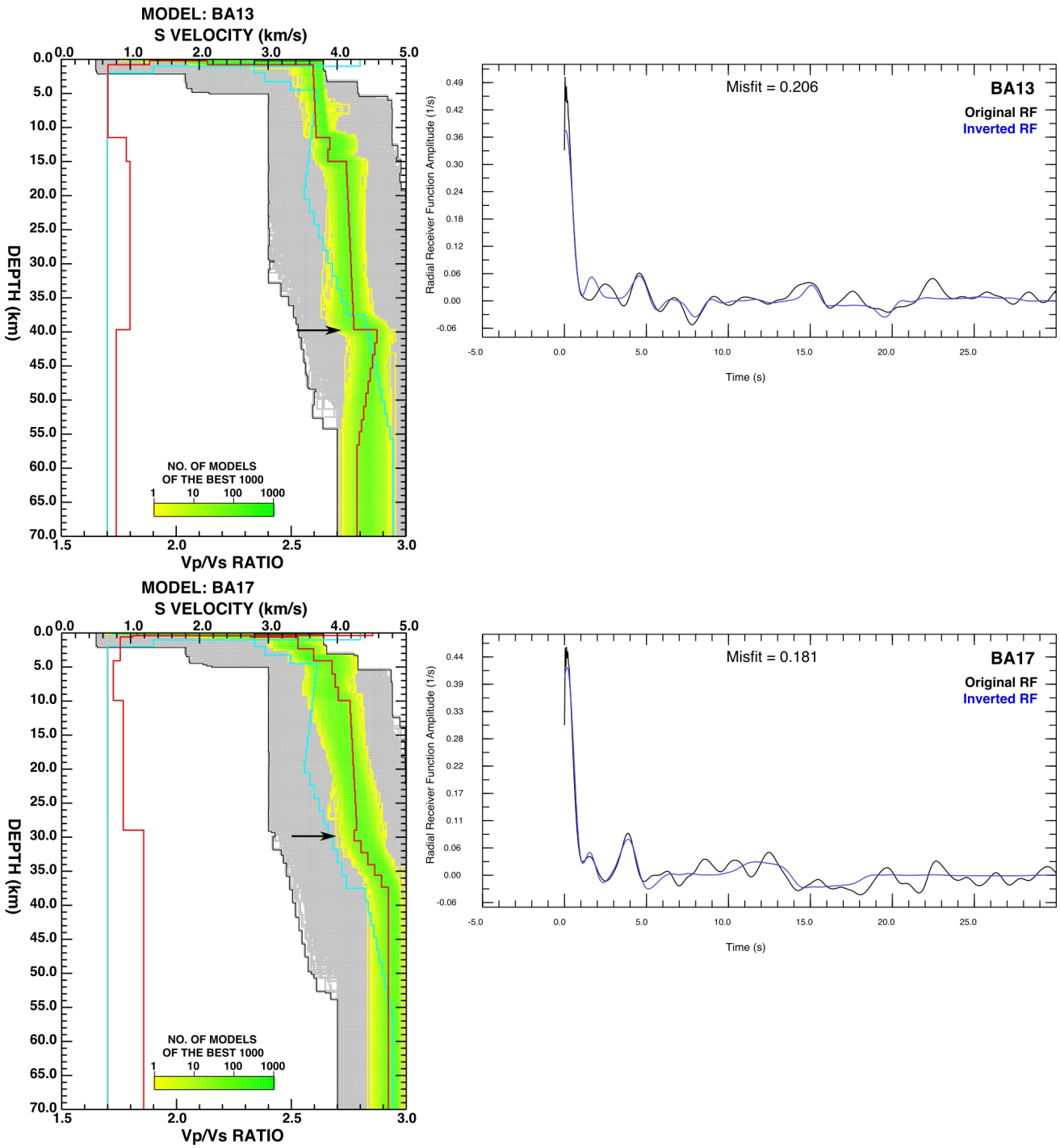

Figure S7: (Left) Density plot of S-wave velocity models and (right) observed and synthetic RF plots for stations BA13 and BA17. Small black arrows on the depth profiles denote the estimated depth of the Moho. Note that receiver function inversion was limited to fitting the waveform between 0 and 30 seconds after the P-arrival for temporary BASS network stations (network code starting with BA) because this produced superior results to the -5 – 30 second time window used for permanent station data. The S-wave velocity models for these two stations are also shown in Figure 9.

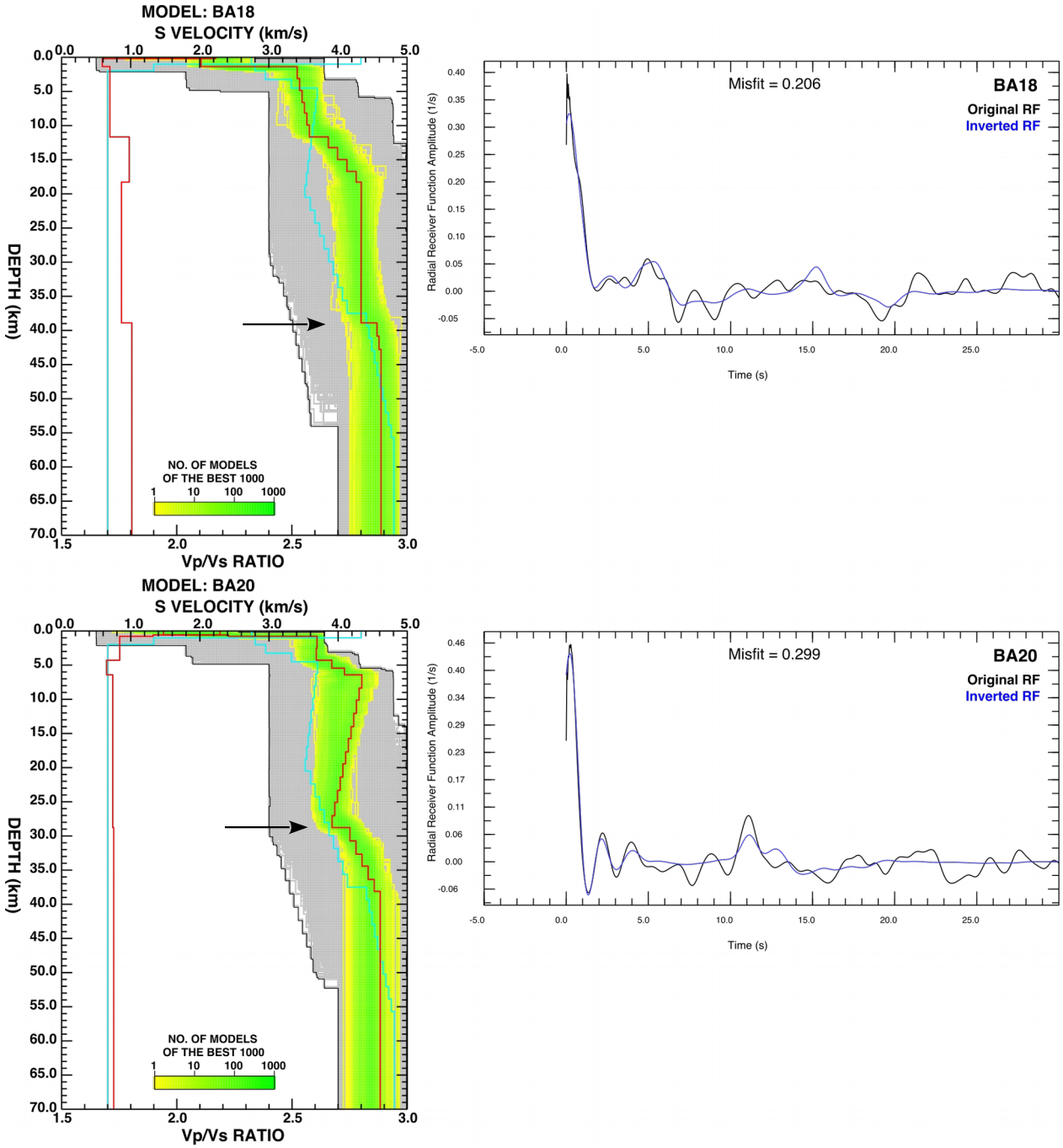

Figure S8: (Left) Density plot of S-wave velocity models and (right) observed and synthetic RF plots for stations BA18 and BA20. Small black arrows on the depth profiles denote the estimated depth of the Moho. Note that receiver function inversion was limited to fitting the waveform between 0 and 30 seconds after the P-arrival for temporary BASS network stations (network code starting with BA) because this produced superior results to the -5 – 30 second time window used for permanent station data.

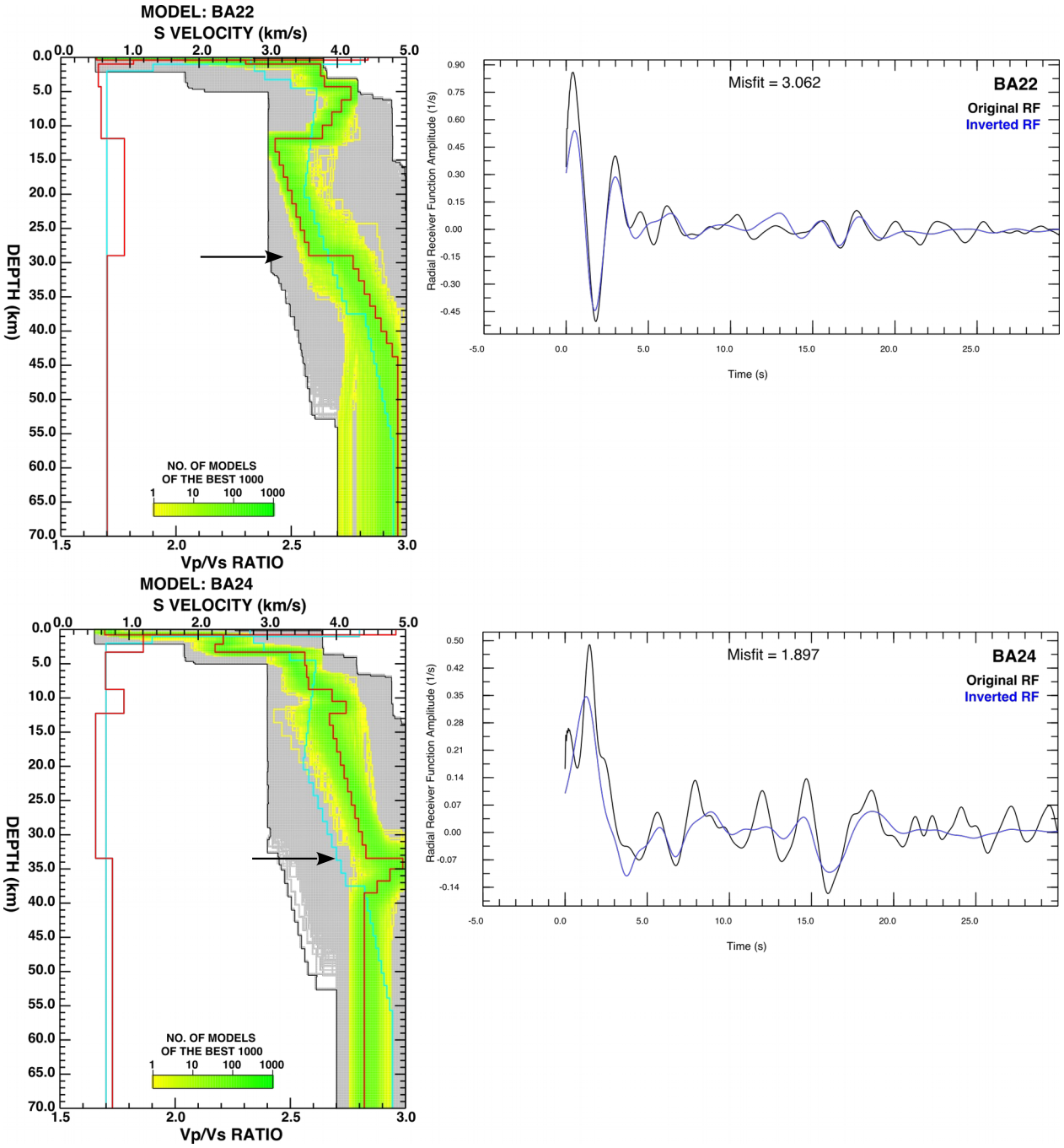

Figure S9: (Left) Density plot of S-wave velocity models and (right) observed and synthetic RF plots for stations BA07 and BA09. Small black arrows on the depth profiles denote the estimated depth of the Moho. Note that receiver function inversion was limited to fitting the waveform between 0 and 30 seconds after the P-arrival for temporary BASS network stations (network code starting with BA) because this produced superior results to the -5 – 30 second time window used for permanent station data.

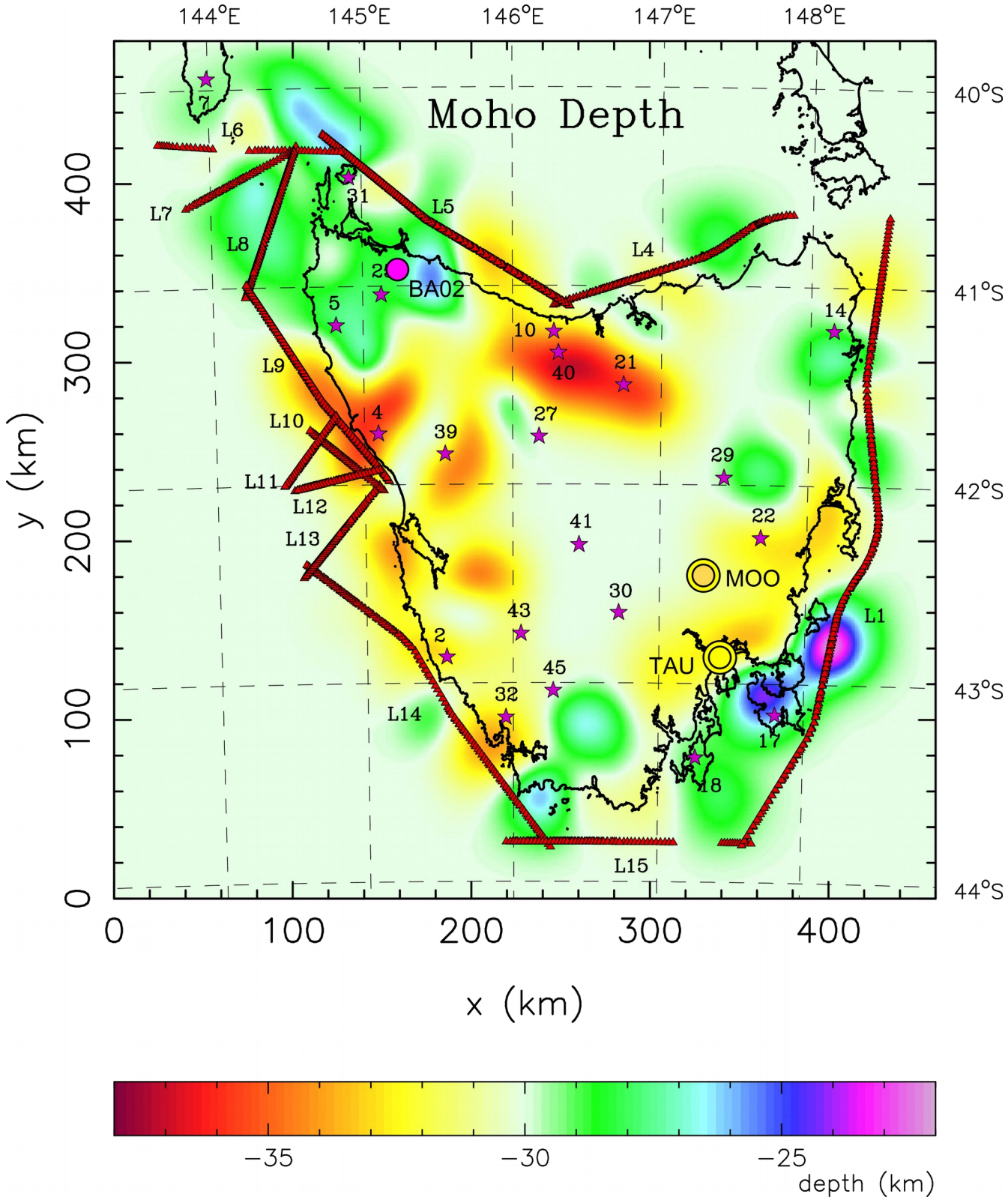

Figure S10: Comparison between Moho map of Rawlinson et al. (2001) and receiver function results from this study. Small circles correspond to results from H-κ stacking, and large circles correspond to results from NA inversion. Contiguous small red triangles denote shot lines (Lines 1-15) and magenta stars denote the location of portable seismic stations (a total of 45, but only those which recorded usable data are shown).